

Article

Mechanical Properties of Rubberised Concrete Confined with Basalt-Fibre Textile-Reinforced Mortar Jackets

Ioanna Skyrianou ^{*}, Lampros N. Koutas and Christos G. Papakonstantinou ^{*}

Laboratory of Concrete Technology & Reinforced Concrete Structures, Department of Civil Engineering, University of Thessaly, GR-38334 Volos, Greece

^{*} Correspondence: iskyrianou@uth.gr (I.S.); cpapak@uth.gr (C.G.P.)

Abstract: This paper presents an experimental investigation of the mechanical properties of rubberised concrete confined with basalt-fibre textile-reinforced mortar (TRM) jackets. The main aim is to evaluate the effectiveness of the TRM confinement scheme on cylindrical rubberised concrete specimens by examining five different mixtures (rubber content ranging from 10.5% up to 42% of the total aggregate volume), including a plain concrete reference mixture. Unconfined and confined specimens with either one or two TRM layers were subjected to monotonic axial loading. The results indicate a decrease in the compressive strength of unconfined concrete as the rubber content increased. The stress–strain curves of rubberised concrete became smoother at the peak as the rubber content increased, also exhibiting increased axial strain capacity post-peak. Rubberised concrete exhibited less brittle failure than plain concrete, accompanied by increased lateral dilation. Confinement with TRM increased the compressive strength, while also enhanced the performance in terms of toughness and axial deformation capacity compared to unconfined concrete. Overall, it is concluded that there is a promising potential for using TRM-confined rubberised concrete in applications with ductility demands and low environmental footprint specifications.

Keywords: rubberised concrete; end-of-life tyres; confinement; TRM; inorganic matrix; basalt textile



Citation: Skyrianou, I.; Koutas, L.N.; Papakonstantinou, C.G. Mechanical Properties of Rubberised Concrete Confined with Basalt-Fibre Textile-Reinforced Mortar Jackets. *Constr. Mater.* **2022**, *2*, 181–199. <https://doi.org/10.3390/constrmater2030013>

Received: 16 June 2022

Accepted: 5 August 2022

Published: 10 August 2022

Publisher's Note: MDPI stays neutral with regard to jurisdictional claims in published maps and institutional affiliations.



Copyright: © 2022 by the authors. Licensee MDPI, Basel, Switzerland. This article is an open access article distributed under the terms and conditions of the Creative Commons Attribution (CC BY) license (<https://creativecommons.org/licenses/by/4.0/>).

1. Introduction

Greenhouse gas emissions from the construction industry are estimated at 5–12% of total national emissions in the EU, while the recovery and recycling of materials could save up to 80% of the aforementioned emissions, according to the European commission [1]. In order to reduce those emissions, promote sustainability and circular economy, the EU has established a framework about waste management [2], also prompting the use of recycled materials in construction [3]. Such a material is granulated rubber recovered from end-of-life tyres. The disposal of end-of-life tyres in landfills poses a serious threat for both the environment and public health, as waste rubber is not biodegradable [4]. On the other hand, rubber can be recycled and reused as crumbs in road construction [5], in asphalt mixtures or for soundproofing. As part of the recycling process, steel wires and textile fabrics are also recovered and can be reused [6]. According to recent statistics [7], 91% of end-of-life tyres are being recycled and reused in the European Union; 61.75% is used for material recovery and 32.85% is used as fuel in the energy production. However, there is still a high-energy demand and high overall cost of the recycling process of waste tyres, which raises concerns about the viability of the methods used [8], especially since the demand and applications of rubber particles are not yet established.

Various approaches for engaging recycled materials in construction have been considered, such as using them as alternatives for cement or as aggregate in concrete. Considering the benefits of reusing rubber waste in the construction industry, the latter approach was selected and rubberised concrete, also called crumb rubber concrete, was first introduced in the early 1990s by the research community. This alternative concrete utilises recycled rubber

as aggregate, yet it is not widely accepted. The main reason is that early studies [9,10] reported that the incorporation of rubber in concrete severely diminished the compressive strength. The reduction in compressive strength was reported to reach up to 80–90% in high rubber contents. Similar reduction trends have been reported for tensile and flexural strength [11], while rubberised concrete has also exhibited improved resistance to abrasion, impact and fatigue [12]. Rubberised concrete also had lower workability and slump than plain concrete, but still within acceptable values for casting [13]. Higher rubber content and fine rubber particles seemed to result in a greater reduction in workability [14]. The incorporation of rubber in concrete also led to a lower density, especially when coarser particles were used, as well as increased air content due to its hydrophobic nature. However, in some cases, segregation and bleeding were reported when the rubber content increased [15]. These significant variations in its properties are possibly attributed to the low stiffness and hydrophobic nature of rubber particles, which result in a weak Interfacial Transition Zone (ITZ) and poor bond between the concrete matrix and rubber particles [9].

A point of interest is the stress–strain behaviour of rubberised concrete. In a typical stress–strain diagram, the incorporation of rubber seemed to increase the axial strain capacity. However, the simultaneous decrease in stiffness and compressive strength resulted in a decreased axial strain at the peak when compared to plain concrete [9,10,12]. Higher rubber contents led to extensive increase in lateral strain with notable lateral dilation of the specimens, as rubber tends to expand more than concrete due to its higher Poisson's ratio, and coarse rubber particles enhanced this effect. Hence, rubberised concrete exhibited less brittle failure compared to plain concrete [12]. Another important factor is toughness. In plain concrete, a primarily brittle material, the plastic energy capacity is low. It has been observed that the incorporation of rubber in concrete increased the energy absorption capacity, leading to higher deformation upon failure and higher toughness [9,10]. However, in high rubber concentrations, toughness was observed to decrease due to the high reduction in compressive strength [16].

The changes in the fresh and mechanical properties of rubberised concrete have led to extensive research for the optimisation of the mixture design. Admixtures such as fly ash and silica fume and the optimisation of the cement, water, rubber and (super-)plasticiser contents have been investigated [15]. Additionally, rubber surface treatment has been evaluated as a solution for the poor adhesion of rubber particles, but without considerable improvement in performance [17,18]. Fibre reinforcement has also been considered as a means to improve the performance of rubberised concrete. For this purpose, the incorporation of recycled steel fibres was investigated. The incorporation of steel fibres had a minimal effect in the compressive strength, but mitigated the decrease in tensile and flexural strength of rubberised concrete [19–21]. However, the toughness was further enhanced when steel fibres were included [22].

The last 5–6 years of research have been focused on the strengthening of rubberised concrete in order to mitigate the reduction in compressive strength and take advantage of its increased energy dissipation properties. Composite materials such as fibre-reinforced polymer (FRP) jackets have been successfully used to confine cylindrical prisms and columns under monotonic and cyclic loading. Although limited studies have been conducted to date, all of them reached to similar conclusions; confinement was more effective in increasing the compressive strength and ultimate axial strain in rubberised concrete for an increasing rubber content. The increase in FRP layers further enhanced both the compressive strength and ultimate axial strain [23–28]. A possible explanation is that the increased lateral dilation of rubberised concrete increases the confinement stresses that act upon the FRP jackets. FRP-confined rubberised concrete indicated explosive failure mode, governed by prominent volumetric expansion. Tests under cyclic loading suggested promising potential for FRP-confined rubberised concrete when high deformability is required. Compared to confined plain concrete elements, major differences were observed in the hysteretic behaviour and energy dissipation of the plastic hinge regions [29–32]. Rubberised concrete columns had a slightly lower drift than plain concrete columns, but higher energy dissipa-

tion and delayed rebar yielding at the same drift level as the plain concrete ones. The axial loading of columns was also found to play an important role on the effectiveness of the confinement scheme.

However, to the best of the authors' knowledge, no other alternative composite materials have been studied as a means of confinement for rubberised concrete elements. Lately, the so-called textile-reinforced mortar (TRM) has been introduced as an alternative to FRP in order to overcome the disadvantages of the organic matrix of the latter, such as poor performance in elevated temperatures and high cost. In contrast, textile-reinforced mortars employ inorganic matrices, usually cement-based, combined with fibre meshes [33]. The confinement of concrete via TRM jackets has proved to be effective in increasing both the compressive strength and axial strain capacity of concrete, especially as the number of layers increase [34,35]. It was reported that the effectiveness of TRMs was lower than FRPs in confining concrete cylinders [34,36], but only slightly lower for concrete columns [37]. The most important differences are that TRMs showed less brittle failure mode and were highly affected by the mechanical properties of the matrix.

Since TRMs have not been used to date for the confinement of rubberised concrete, this study aims to assess a novel strengthening scheme that utilises TRM jackets as a means of confinement. The mechanical performance of four trial rubberised concrete mixtures was evaluated and compared with a reference plain concrete mixture. Both unconfined and basalt TRM-confined cylindrical specimens were subjected to monotonic axial loading. The possibility of developing a sustainable construction material that can be used when high deformability is required is also investigated.

2. Materials and Methods

Five trial concrete mixtures were examined, one plain concrete mixture as reference and four rubberised concrete mixtures, in which part of the mineral aggregates were replaced by rubber particles by volume. From each mixture 8 specimens remained unconfined, while 3 were confined with 1 TRM layer and 3 with 2 TRM layers. The plain concrete mixture was denoted by "Control Mix—CM" and rubberised concrete mixtures were denoted by "RX"; the use of rubber was denoted by the letter R, while the aggregate replacement ratio was denoted by the number X. Unconfined specimens were denoted by the abbreviation "Unc", while confined specimens were denoted by the abbreviation "1L" or "2L", for 1 or 2 TRM layers, respectively.

Type II Portland cement with a characteristic strength of 42.5 MPa and crushed limestone aggregate (hereafter referred to as mineral aggregate) with a nominal maximum size of 16 mm was used for all the concrete mixtures. The aggregates were sieved in six gradations for the purposes of this study (Figure 1a). Rubber particles obtained from the tyre-recycling plant Retire ABEE in Drama Greece were used. Their size varied from 2–8 mm and they were sieved in two gradations, 2–4 mm and 4–8 mm, to match the mineral aggregate ones (Figure 1b). The bulk density of the rubber particles was approximately 1/3 of that of the mineral aggregates, as measured in the lab. A superplasticiser was also used in all mixtures to improve the workability of fresh concrete.

A plain concrete mixture (CM) was designed according to the grade distribution limits set in the Greek Concrete Technology Code 2016 [38], as presented in Figure 2. When designing the mixtures, the possibility of water absorption from the dry mineral aggregate was also considered, and more water was added in the final mixture. Hence, the water to cement ratio (w/c) was equal to 0.397 for all mixtures. The proportions of each concrete mixture are presented in Table 1. In rubberised concrete mixtures, two of the fine aggregate particle sizes (2–4 mm and 4–8 mm) were replaced by a volume with rubber particles of the same size with replacement ratios of 25% (mixture R25), 50% (mixture R50), 75% (mixture R75) and 100% (mixture R100). Therefore, the rubber particles comprised 10.5%, 21%, 31.5% and 42% of the total aggregate volume in mixtures R25, R50, R75 and R100, respectively (Figure 3).



Figure 1. Sieved gradations of the (a) mineral aggregate and (b) rubber particles.

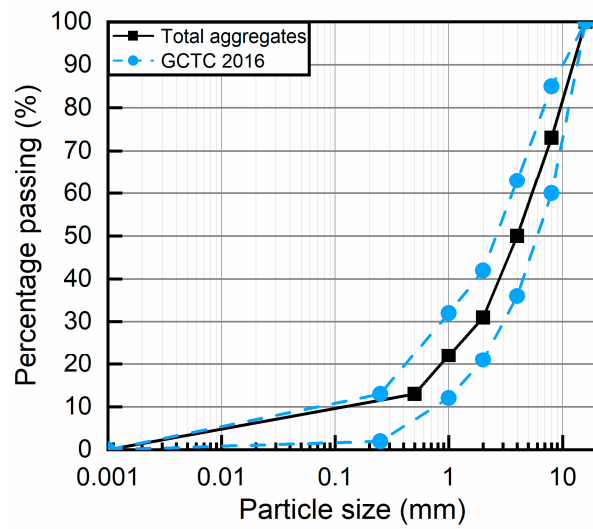


Figure 2. Particle size distribution of the total aggregate and GCTC 2016 boundaries.

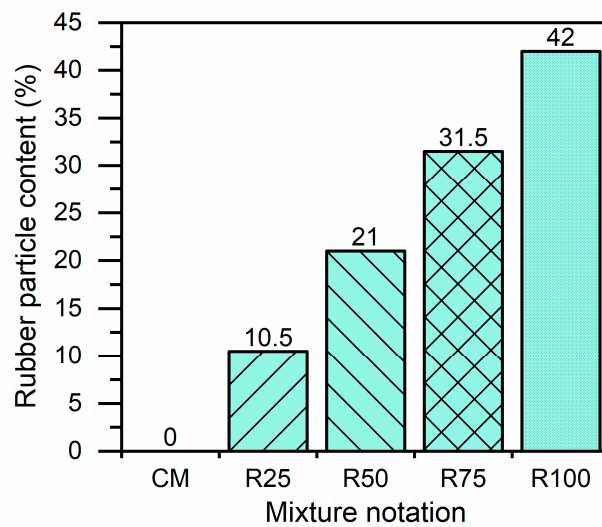


Figure 3. Content of the rubber particles of the total aggregate volume.

Table 1. Proportions of all concrete mixtures [kg/m³].

| Material | Mixture Notation | | | | |
|-------------------|------------------|-------|-------|-------|-------|
| | CM | R25 | R50 | R75 | R100 |
| Cement | 365.8 | 365.8 | 365.8 | 365.8 | 365.8 |
| Water | 145.2 | 145.2 | 145.2 | 145.2 | 145.2 |
| Mineral aggregate | 8–16 mm | 507.9 | 507.9 | 507.9 | 507.9 |
| | 4–8 mm | 432.7 | 324.5 | 216.3 | 108.2 |
| | 2–4 mm | 357.5 | 268.1 | 178.8 | 89.4 |
| | 1–2 mm | 169.3 | 169.3 | 169.3 | 169.3 |
| | 0.5–1 mm | 169.3 | 169.3 | 169.3 | 169.3 |
| | 0–0.5 mm | 244.6 | 244.6 | 244.6 | 244.6 |
| Rubber particles | 4–8 mm | 0 | 36.1 | 72.1 | 108.2 |
| | 2–4 mm | 0 | 29.8 | 59.6 | 89.4 |
| Superplasticiser | 2 | 2 | 2 | 2 | 2 |

A concrete mixer with 200 L capacity was used. The mixing procedure of the rubberised concrete began by gradually adding each gradation of mineral aggregate and the rubber particles and dry mixing for approximately 1 min to ensure a good distribution. The cement was then added to the concrete and dry mixed for another minute. The superplasticiser was diluted in the water, which was added gradually to the mixture. The concrete was mixed for another 2–3 min until it reached the required consistency. The preparation of the specimens was performed according to EN 12390–2:2019 [39]. The concrete was poured into plastic moulds to prepare cylindrical specimens of 100 mm diameter and 200 mm height. All moulds were filled with fresh concrete in three equal layers, while each layer was compacted using a steel rod. The free surface was finished using a trowel. All specimens were left to harden for a minimum of 24 h before removing from the moulds. Hardened specimens were left to cure in air at least 14 days in ambient environment conditions before the application of the TRM confinement.

To evaluate the workability of the fresh concrete, slump and air content were measured for each mixture. A slump test was performed using a standard Abrams cone according to EN 12350-2:2019 [40]. An air content test was performed using a hydraulic pressure apparatus as determined by EN 12350-7:2019 [41]. After hardening, the bulk density of hardened concrete was determined according to EN 12390-7:2019 [42].

TRM confinement was applied in 6 specimens from each mixture; 3 specimens were confined with 1 TRM layer and 3 with 2 TRM layers, totalling in 30 confined specimens from all five mixtures. A two-directional coated basalt-fibre textile with a 6 mm square mesh was used for the TRM jackets. The particular mesh size was considered more suitable for the size of the cylindrical specimens used in this study. The properties of the basalt textile according to the manufacturer’s datasheets are presented in Table 2. A commercially available cementitious mortar was used as matrix, comprising a water to binder ratio of 0.23. The dry binder contained fine aggregates with a maximum size of 1.3 mm and microfibres made of polypropylene. The strength of the mortar was found through flexural and compressive tests on three 40 mm × 40 mm × 160 mm mortar prisms according to EN 1015-11:2019 [43]. The average values of the compressive and flexural strength were 22.59 MPa and 4.02 MPa, respectively.

Table 2. Properties of basalt textile.

| Mesh Size | Weight with Coating | Equivalent Thickness | Tensile Strength | Modulus of Elasticity | Failure Strain |
|-------------|----------------------|----------------------|------------------|-----------------------|----------------|
| 6 mm × 6 mm | 250 g/m ² | 0.039 mm | 1542 MPa | 89 GPa | 1.8% |

For the jacket application, the following procedure was followed: (a) a first layer of mortar was applied on clean and dampened concrete surface; (b) the textile was pressed in the mortar and wrapped around the cylinder in either one or two layers, including an overlapping zone equal to 1/3 of the specimen's circumference (Figure 4); (c) additional mortar was applied in between the layers and a final mortar layer was applied to completely cover the textile; and (d) extra confinement was provided near the edges of the cylinders (20 mm wide basalt textile strips) to prevent local concrete crushing due to stress concentration. As a part of the curing process of the jackets, the specimens were immersed in water for one minute for two consecutive days after the hardening of the jackets. Then, specimens were left to cure in air in ambient environment conditions for at least 28 days before testing.



Figure 4. Application of the TRM jacket.

Before testing, all specimens were capped with gypsum to ensure the levelness of the testing surface. Potentiometers were used to record axial deformations in the majority of specimens. Two potentiometers (POT A and POT B) were attached parallel to the specimen's longitudinal axis and placed diametrically opposed, as presented in Figure 5. The compression tests were carried out using a 3000 kN capacity testing machine with a constant displacement rate of 15 $\mu\text{m/s}$. Data were recorded using a fully automated data acquisition system.

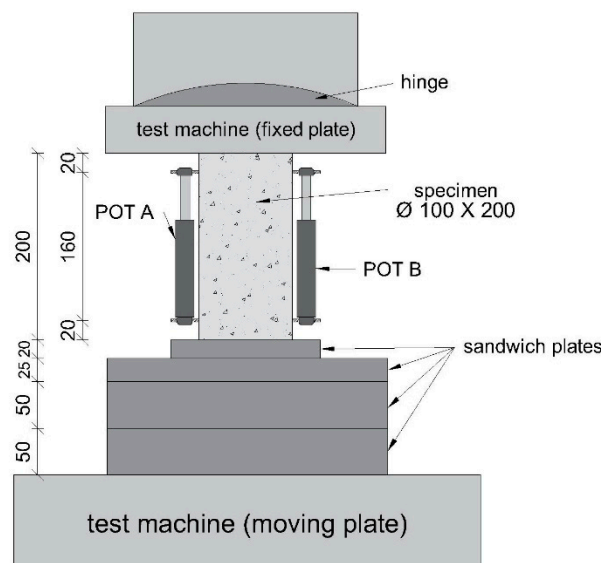


Figure 5. Test configuration (dimensions in mm).

3. Results and Discussion

3.1. Fresh and Physical Properties

The results of the fresh and physical properties of the concrete mixtures are presented in Table 3. Contrary to previous studies [13–15], the slump was not found to be significantly affected by the increasing rubber content except for mixture R100. This differentiation in results is probably due to the use of a superplasticiser. Hence, mixtures CM, R25, R50 and R75 had a similar collapsed slump which ranged from 150 to 165 mm. On the contrary, in mixture R100, the slump value was reduced significantly to 65 mm, thus exhibiting a decrease of 57% compared to the plain concrete mixture. In this case, rubber particles comprise 42% of the total aggregate volume; they have a higher surface area than mineral aggregates and the friction in fresh concrete increased resulting in reduced workability.

Table 3. Results of the fresh and physical properties.

| Mixture Notation | Slump [mm] | Air Content [%] | Bulk Density [kg/m ³] |
|------------------|------------|------------------|-----------------------------------|
| CM | 150 | 2.8 | 2512.0 |
| R25 | 155 | 2.2 | 2383.6 |
| R50 | 165 | 2.4 | 2206.4 |
| R75 | 160 | 3.9 | 2133.7 |
| R100 | 65 | n/a ¹ | 1956.8 |

¹ Data not available.

Entrained air increased up to 39% as the rubber content increased. This is in accordance with previous studies [15,18,21], as the hydrophobicity of rubber particles entraps air around them. Indicative of the increased air content of rubberised concrete mixtures with high rubber content was the apparent porosity in the specimens' surface. Additionally, the bulk density of hardened concrete was reduced up to 22% with the incorporation of rubber particles. This is mainly due to the lower density of rubber particles. Additionally, the increased porosity and air voids in the rubberised concrete further decreased the density. The overall decrease in density results in substantially reduced weight in rubberised concrete members. This is a favourable property, particularly in the case of seismic loading because it will lead to a reduced seismic mass.

3.2. Mechanical Properties

The experimental results related to the mechanical properties are summarised in Table 4. Compressive strength was found as the average from eight tested unconfined specimens, and from three confined ones per investigated parameter. Deformation data were acquired from three specimens per mixture. Toughness was calculated as the area under the stress–strain curve until the moment of failure of the specimens. Failure was decided by the authors as the point where the stress dropped by 20% after the peak.

3.2.1. Compressive Strength

The statistical analysis of the concrete compressive strength was performed using the statistical program SPSS Statistics (v. 27). The effect of rubber content (CM, R25, R50, R75 and R100) and type of confinement (0L, 1L and 2L) on concrete strength was explored with a 5 × 3 ANOVA with rubber content and confinement as the between-subjects factors. Post hoc comparisons using Tukey's method were conducted when necessary. Data are presented as mean values (±SEM) and are plotted by rubber content in Figure 6. Statistical significance was set at a <0.05.

Table 4. Results of the mechanical properties of the rubberised concrete. Numbers in parentheses refer to the standard deviation.

| Mixture Notation | Compressive Strength [MPa] | Strain at Peak [%] | Toughness [10^4 J/m ³] |
|------------------|----------------------------|--------------------|---------------------------------------|
| Unc_CM | 33.70 (2.91) | 2.120 (0.24) | 5.645 (0.98) |
| Unc_R25 | 18.86 (1.97) | 1.672 (0.30) | 3.121 (0.57) |
| Unc_R50 | 11.25 (1.38) | 1.285 (0.10) | 1.829 (0.05) |
| Unc_R75 | 9.30 (0.47) | 1.935 (0.78) | 2.235 (1.26) |
| Unc_R100 | 7.39 (0.52) | 1.591 (0.78) | 2.220 (0.22) |
| 1L_CM | 39.01 (2.07) | 1.811 (0.29) | 5.454 (1.09) |
| 1L_R25 | 24.79 (1.32) | 1.740 (0.54) | 4.217 (0.78) |
| 1L_R50 | 15.18 (1.06) | 2.543 (0.69) | 4.571 (0.80) |
| 1L_R75 | 12.41 (0.35) | 1.190 (0.39) | 14.677 (1.37) |
| 1L_R100 | 10.01 (0.66) | 1.736 (0.32) | 12.316 (2.99) |
| 2L_CM | 41.00 (3.63) | 2.314 (0.14) | 11.492 (2.04) |
| 2L_R25 | 24.99 (1.18) | 1.649 (0.29) | 23.622 (1.72) |
| 2L_R50 | 14.45 (0.71) | 2.325 (0.77) | 39.642 (1.25) |
| 2L_R75 | 12.23 (0.41) | 1.427 (0.38) | 41.020 (3.62) |
| 2L_R100 | 10.21 (0.29) | 1.672 (0.54) | 29.085 (5.93) |

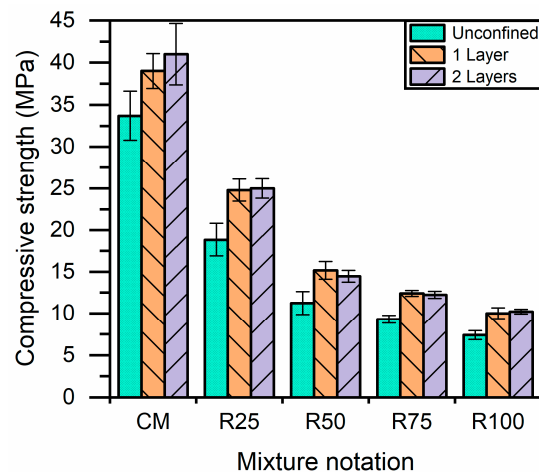


Figure 6. Compressive strength of the rubberised concrete mixtures.

As suggested by previous studies [9,10,13,14], the compressive strength of unconfined rubberised concrete decreased for an increasing rubber content, and in some cases, the decrease was up to 85%. The statistical analysis of concrete compressive strength revealed a significant main effect of rubber content ($F(4, 53) = 569.92, p < 0.001, \text{partial } \eta^2 = 0.98$). Post hoc comparisons revealed that increasing the rubber content decreased compressive strength (CM: 37.90 ± 0.49 , R25: 22.88 ± 0.48 , R50: 13.63 ± 0.48 , R75: 11.32 ± 0.48 , R100: 9.21 ± 0.53 , CM vs. R25 vs. R50, R75 vs. R100; $p < 0.05$). Replacing mineral aggregates with rubber particles reduced the compressive strength by 44.1%, 66.6%, 72.4% and 78.1% for mixtures R25, R50, R75 and R100, respectively (Figure 6), signifying the severe impact of incorporating rubber particles in concrete. The poor adhesion of the rubber particles with the cement paste and the high porosity of the mixture further reduced the compressive strength. The reduction rate was higher up to mixture R50 due to the rubber content increasing up to the point where the rubber particles highly affect the concrete’s behaviour [19].

Confinement with 1 TRM layer increased the compressive strength by 15.8% for CM and to 35.5% for R100. In the case of two TRM layers, the increase was 21.7% for

CM and 38.1% for R100 (Figure 6). The statistical analysis indicated that confinement also significantly affected strength ($F(4, 53) = 154.45, p < 0.001, \text{partial } \eta^2 = 0.69$). More specifically, specimens confined by one or two layers exhibited a higher strength compared to the unconfined specimens (0L: 16.1 ± 0.26 vs. 1L: 20.28 ± 0.42 and 0L: 16.1 ± 0.26 vs. 2L: $20.58 \pm 0.44; p < 0.001$). Similar to what has been reported for FRP confinement [25,28], the effectiveness of the TRM confinement was enhanced for a higher rubber content, as the increased lateral dilation caused by the rubber particles led to the earlier activation of the TRM jackets. The de-creasing trend of the compressive strength was comparable to that of the unconfined specimens as the rubber content increased.

Interestingly, no significant difference was found between specimens confined with one or two layers (1L: 20.28 ± 0.42 vs. 2L: $20.58 \pm 0.44; p > 0.05$) (see Figure 6). The confinement effect was similar to all concrete specimens regardless of the rubber content, as implied by the non-significant “rubber content \times confinement type” interaction ($F(8, 53) = 2.1, p > 0.05$). More specifically, confinement with two TRM layers did not significantly increase the compressive strength (increase up to 5%) when compared with one TRM layer-confined specimens. This is attributed to the late activation of the jackets and their early failure at one of the two ends of the cylindrical concrete specimens; the provided additional confinement at the two ends proved to be inadequate.

3.2.2. Stress–Strain Behaviour

Typical stress–strain curves for the unconfined and confined specimens are presented in Figures 7 and 8, respectively. Failure is marked on each curve at the drop of stress by 20%. It is evident that the incorporation of rubber in concrete significantly decreased the compressive strength, but also increased the axial strain capacity post-peak by the means of increased ultimate axial strain, although the axial strain at the peak was reduced when compared to plain concrete. Indicative is that plain concrete exhibited strain at the peak around 2‰, while rubberised concrete ranged from 1.3‰ to 1.9‰ and the reduction was greater for mixture R100. It was also observed that the curve progressively became smoother at the peak and the effect was more pronounced as the rubber content increased. Comparable to previous studies [9,10,13], the ultimate axial strain increased as the rubber content increased. This can also be observed when comparing the normalised strain at different stress levels after the peak load, as presented in Figures 9 and 10 for the unconfined and confined specimens, respectively. The axial strain of each mixture is normalised with the strain at peak load. As it is observed in Figure 9, the plain concrete indicated almost no increase in axial strain after the peak as it failed immediately after reaching its maximum stress. When the rubber content increased, the axial strain capacity post-peak of rubberised concrete also increased, especially in higher rubber contents. Indicative of this behaviour is the fact that the specimens failed (denoted by drop of stress by 20%) in higher ultimate strain values than plain concrete, as noted in Figure 9 with an increasing rate. Thus, the rubberised concrete exhibited less brittle behaviour than the plain concrete because of the progressive cracking development.

It is evident that confinement enhanced the compressive strength and further increased the axial strain capacity post-peak in all mixtures. Specifically, the ultimate axial strain ranged from 1.7‰ to 3‰ for unconfined specimens, while confined specimens exhibited an ultimate axial strain of more than 10‰ in most cases. The effect was more pronounced as the rubber content increased. However, in all confined specimens after achieving the peak stress, a significant drop in strength was observed, as presented in Figure 8, due to the late activation of the jackets. As a result, the confinement remained inactive until the concrete core expanded enough laterally in order to activate the jackets. This is probably attributed to the large thickness of the mortar and the inadequate additional confinement provided at the edges. Yet, after the activation, some specimens managed to recover part of the initial lost strength, while all of them exhibited enhanced axial strain capacity post-peak.

When comparing confinement between one and two TRM layers, one will notice very minor differences in terms of overall behaviour. In both cases, when the rubber content

increased, the drop in stress was not as abrupt, since a higher rubber content led to increased lateral expansion, thus resulting in the earlier activation of the jackets. This can also be observed through the comparison of the increase in the axial strain after the peak. For mixtures CM, R25 and R50 confined with one TRM layer, specimens failed almost abruptly, hence the marginal increase in axial post-peak strain (Figure 10a). However, mixtures R75 and R100 indicated a higher axial strain capacity post-peak. The high increase in post-peak strain resembles ductile materials. On the other hand, specimens confined with two TRM layers showed enhanced axial strain capacity post-peak and had a slightly less abrupt loss of strength (Figure 10b). The activation of the jackets was enhanced, therefore leading to a rapid increase in the axial strain post-peak in mixtures R50, R75 and R100.

When comparing the stress–strain curves of the same mixture, it was observed that confinement resulted in a compressive strength and axial strain capacity post-peak increase but not effectively for every mixture. For the plain concrete mixture (CM), the increase in compressive strength is evident, as well as the abrupt stress drop post-peak (Figure 11a). In this case, confinement was activated too late, after the stress was reduced by 20% (where the failure is denoted), meaning that confinement was not totally effective. Mixture R25 (Figure 11b) exhibited a similar behaviour to plain concrete, signifying that the rubber content was relatively low, and specimens did not manage to expand enough laterally in order to activate the jackets. This resulted in a marginal increase in terms of ultimate axial strain, which remained below 5‰. Mixture R50 (Figure 11c) had a better performance when confined with two TRM layers, as strain hardening was observed leading to a high axial strain capacity post-peak, indicating ultimate axial strain on average 27.5‰. Yet, the increase in compressive strength was marginal compared to one TRM layer confinement. The best performance was observed in mixture R75 (Figure 11d) as both confined specimens managed to attain a high axial strain capacity post-peak; the ultimate axial strain was 22‰ and 28‰ on average for one and two TRM layers, respectively. Especially, specimens confined with two layers exhibited strain hardening post-peak and a less abrupt drop of stress. This is probably due to the quicker activation of the jackets, as the specimens with increased rubber content exhibited larger lateral deformations. However, the performance of specimens from mixture R100 (Figure 11e) was inferior when compared to those from mixture R75. This is attributed to the very high rubber content, which significantly decreased compressive strength up to a point where all the mechanical properties of concrete are highly affected by rubber particles. As a result, confined specimens from mixture R100 failed when the ultimate axial strain reached 10‰ and 27‰ on average for one and two layers, respectively.

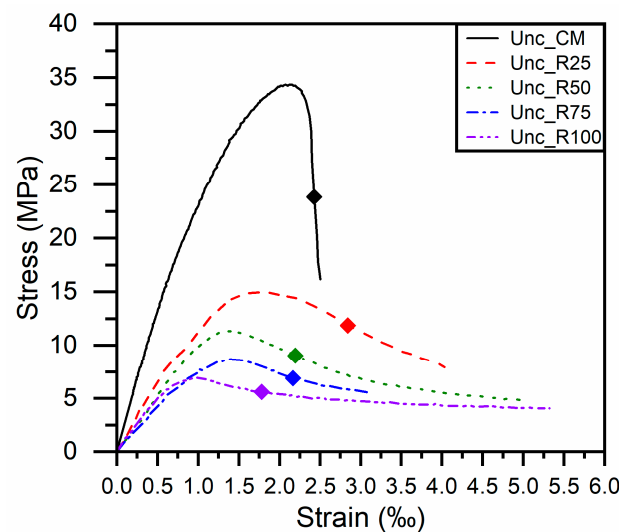


Figure 7. Stress–strain curves of the unconfined specimens. Markers denote failure (20% stress drop).

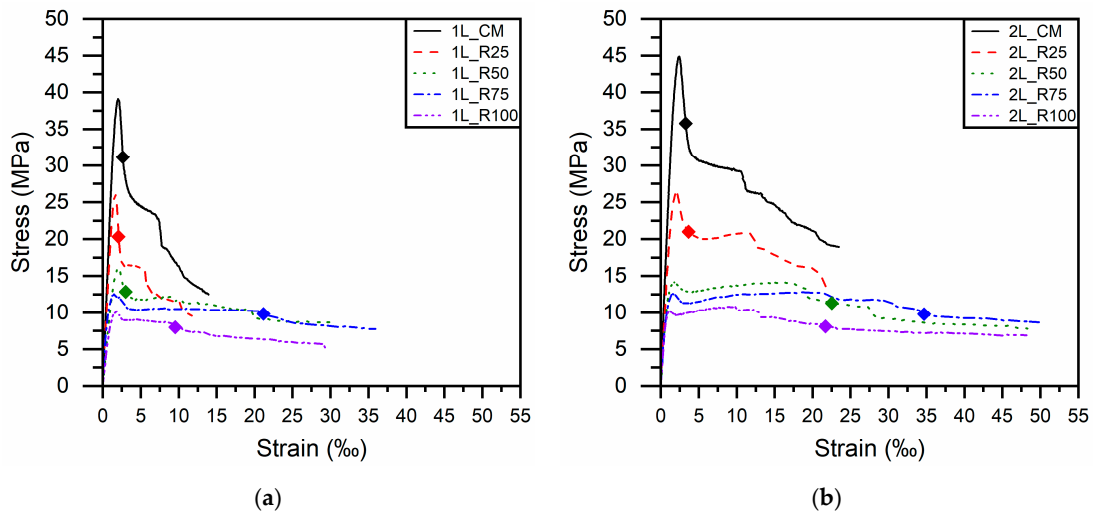


Figure 8. Stress–strain curves of (a) 1 TRM layer- and (b) 2 TRM layer-confined specimens. Markers denote failure (20% stress drop).

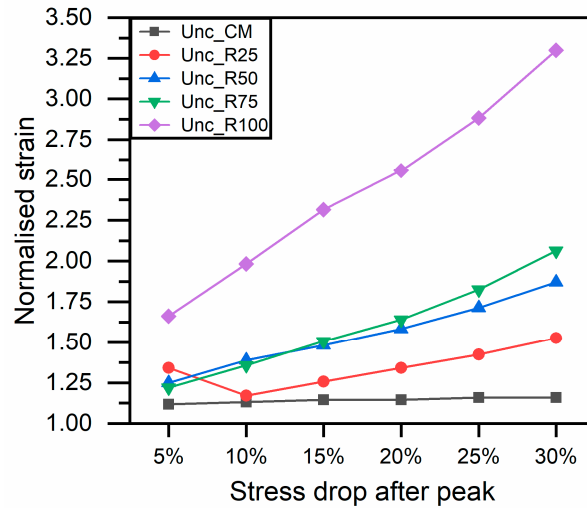


Figure 9. Normalised strain values at different stress drop levels for the unconfined specimens.

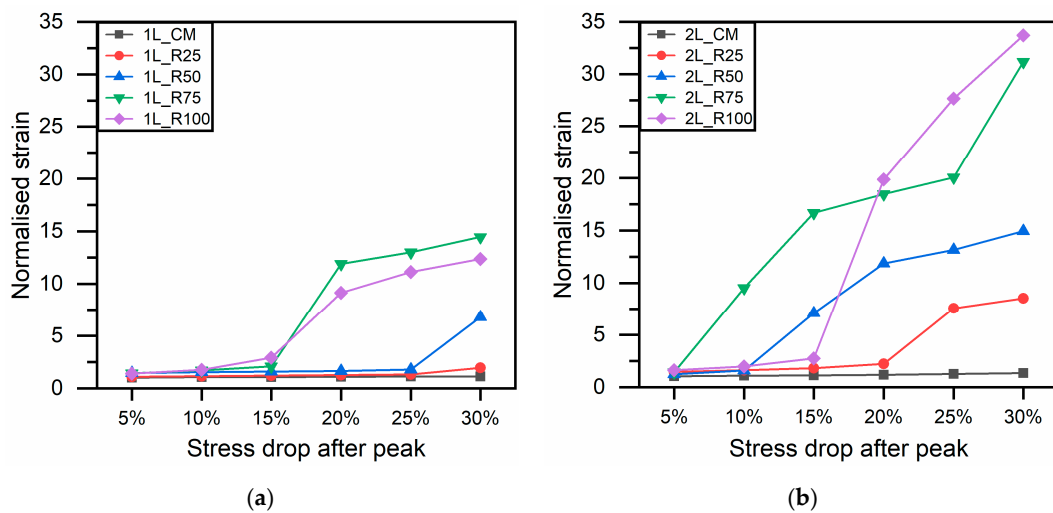


Figure 10. Normalised strain values at different stress drop levels for confined specimens with (a) 1 TRM layer and (b) 2 TRM layers.

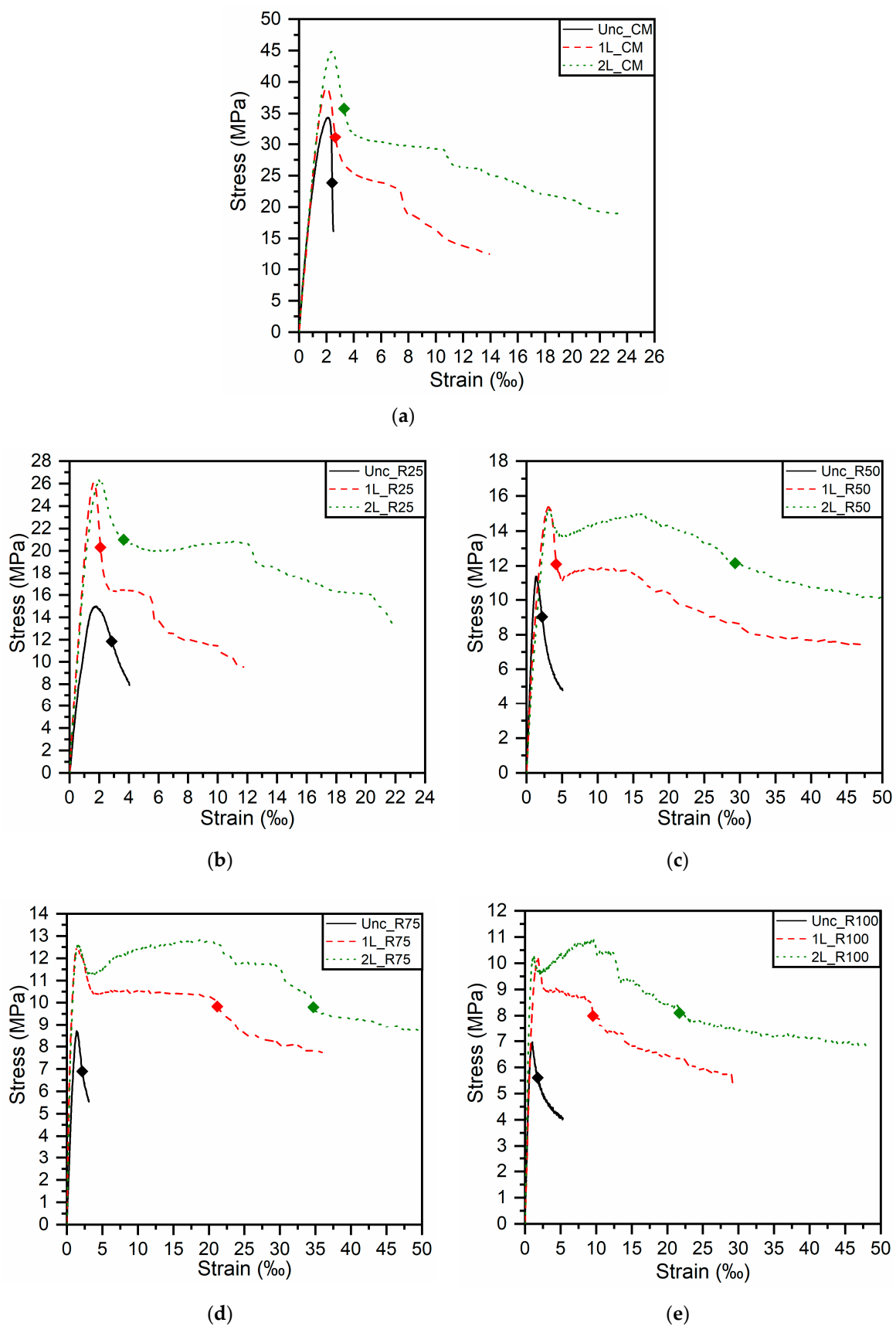


Figure 11. Stress–strain curves of mixtures (a) CM, (b) R25, (c) R50, (d) R75 and (e) R100. Markers denote failure (20% stress drop).

3.2.3. Toughness

The toughness of each mixture was calculated as the area under the stress–strain curve until failure (denoted by drop of stress by 20%). For the unconfined specimens, plain concrete mixture (CM) exhibited the highest toughness, and the rest of rubberised concrete mixtures had similar lower values (Figure 12). This indicates that, despite their higher axial strain capacity post-peak compared to plain concrete, the significant loss of strength prevented rubberised concrete from achieving a high energy absorption capacity.

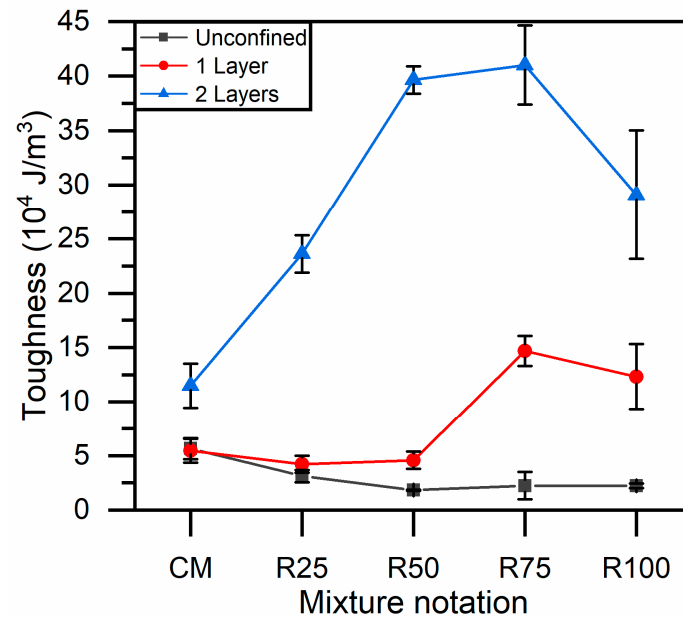


Figure 12. Toughness of rubberised concrete until failure (20% stress drop).

Concerning the specimens confined with one TRM layer, the plain concrete (CM) exhibited a higher toughness than mixtures R25 and R50 by 22.7% and 16.2%, respectively. On the contrary, mixtures R75 and R100 exhibited a higher toughness than plain concrete by 169.1% and 125.8%, respectively. This is attributed to the relatively low axial strain capacity post-peak of the former mixtures. In the case of specimens confined with two TRM layers, the plain concrete exhibited a lower toughness than all the rubberised concrete mixtures. The increase in toughness ranged from 105.6% to 256.9%. In both cases, the rubberised concrete was expected to have a higher toughness due to its increased axial strain capacity post-peak. However, the significant loss of strength due to the high rubber content and early failure of the confinement prevented some specimens from enhancing their toughness and energy absorption capacity. Hence, better results are expected if the optimisation of the mixtures and the confinement scheme are accomplished. Additionally, specimens confined with two TRM layers exhibited a ductile-like behaviour, having increased toughness, an important property when high ductility and/or deformability is required in concrete members.

Table 5 presents the toughness of three different mixtures that exhibit similar compressive strengths and can aid the evaluation of the confinement effect on both compressive strength and toughness. More specifically, the toughness of an unconfined mixture (R50) with a compressive strength of 11.25 MPa is compared to two confined mixtures that exhibit similar compressive strengths of 10.01 MPa and 10.21 MPa. The unconfined specimens from mixture R50, in which rubber particles comprised 21% of the total aggregate volume, had an average compressive strength of 11.25 MPa. When the rubber content was doubled (42% of the total aggregate volume) in mixture R100, the confined specimens with one and two layers had similar compressive strengths, 10.01 MPa and 10.21 MPa, respectively. It is evident that an increase in rubber particles in the mixture reduces the compressive strength, but the confinement can counteract this decrease and provide a significant increase in

toughness. The increase in rubber content in addition to confinement by one or two TRM layers resulted in a toughness increase by 573% and 1490%, respectively. Therefore, the same compressive strength can be achieved while taking advantage of the high toughness provided by the rubber particles when increasing the rubber content, but also applying confinement. That system could be potentially used in applications where high deformability is required, such as columns in seismic-prone areas.

Table 5. Comparison between specimens with similar compressive strengths.

| Specimen ID | Rubber Content [%] | Confinement | Compressive Strength [MPa] | Toughness [10^4 J/m^3] |
|-------------|--------------------|-------------|----------------------------|------------------------------------|
| Unc_R50 | 21 | no | 11.25 | 1.829 |
| 1L_R100 | 42 | 1 layer | 10.01 | 12.316 |
| 2L_R100 | 42 | 2 layers | 10.21 | 29.085 |

3.3. Failure Modes

All unconfined CM specimens exhibited a similar brittle failure as a result of extensive longitudinal cracking; a typical failure mode is presented in Figure 13a. The use of rubber particles altered the failure mode to a more gradual one as the rubber content increased. The incorporation of rubber particles led to an increased number of finer cracks in the specimens, as presented in a typical specimen from mixture R100 in Figure 13b. In high rubber contents, extensive cracking appeared at the top or bottom surfaces of the cylindrical specimens. Additionally, specimens with increased rubber content exhibited larger lateral dilation due to rubber’s high elasticity.

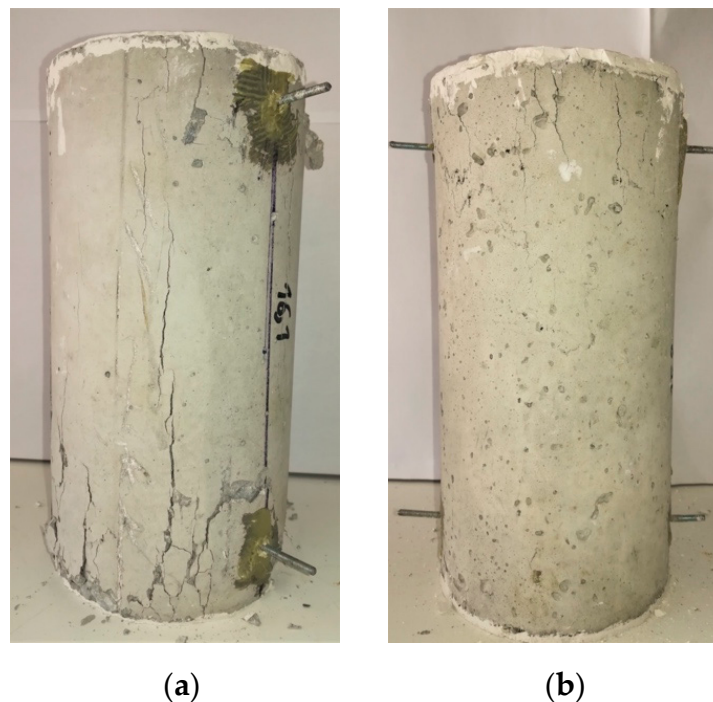


Figure 13. Failure modes of the unconfined specimens from mixtures (a) CM and (b) R100.

The confined specimens failed due to the fibre rupture of the textile. Failure was initiated at one of two ends of the specimens, proving that the provided additional confinement at the edges was inadequate. The typical failure modes of the confined specimens exhibiting fibre rupture are presented in Figure 14, where one can notice the failure at the edge of the jackets. In almost half of the specimens, the debonding of the TRM jacket at the end of the overlap zone was observed as well as fibre rupture. The failure in this case

was also initiated at one edge and progressed towards the middle of the specimen. The typical failure modes of confined specimens, including the debonding of the TRM jacket, are presented in Figure 15. In addition, the confined specimens exhibited notable lateral dilation as the rubber content increased and the effect was further pronounced when two TRM layers were applied.

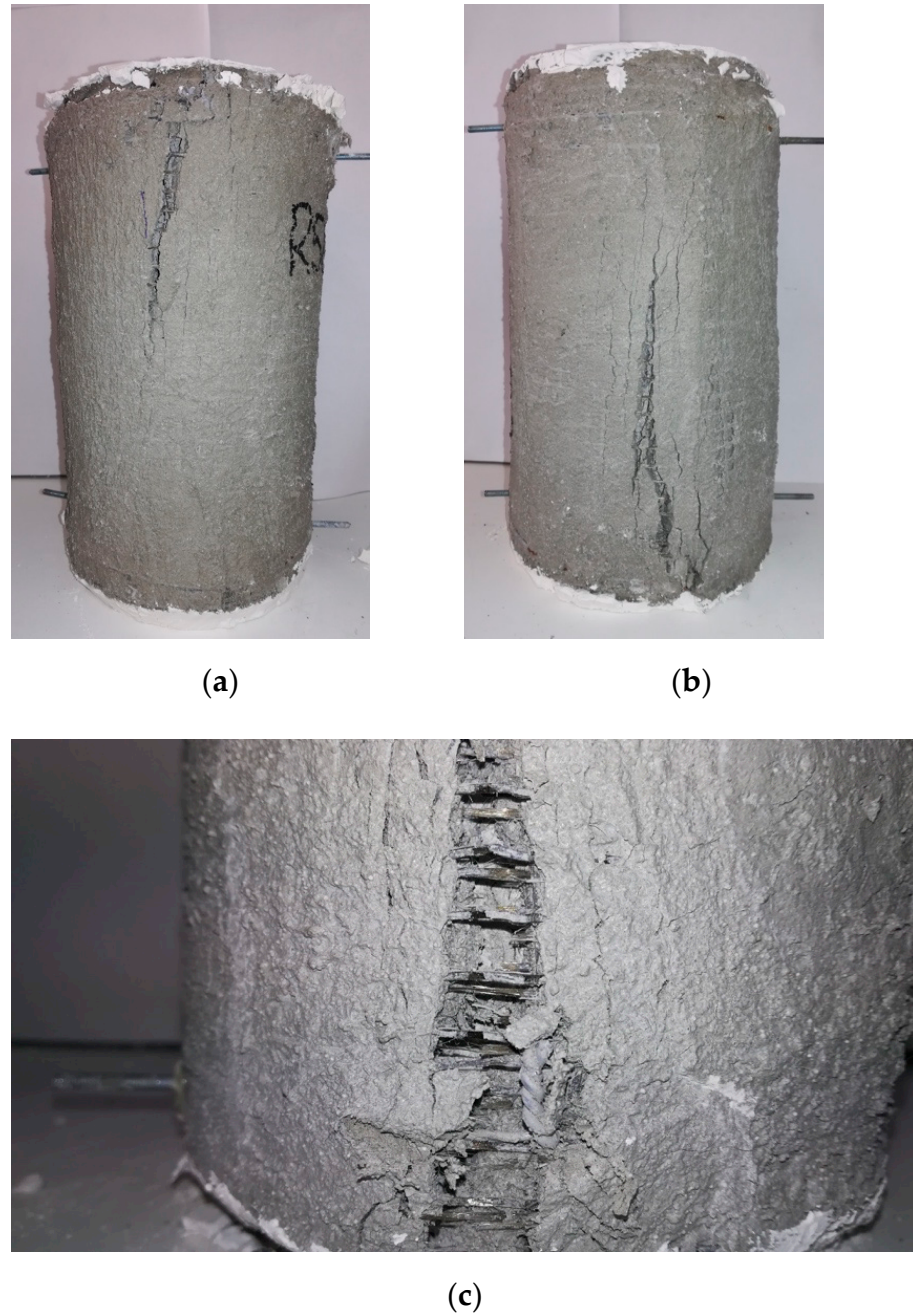


Figure 14. Failure modes of the confined specimens exhibiting fibre rupture from mixture (a) R50_1L; (b) R25_1L and (c) R50_2L.

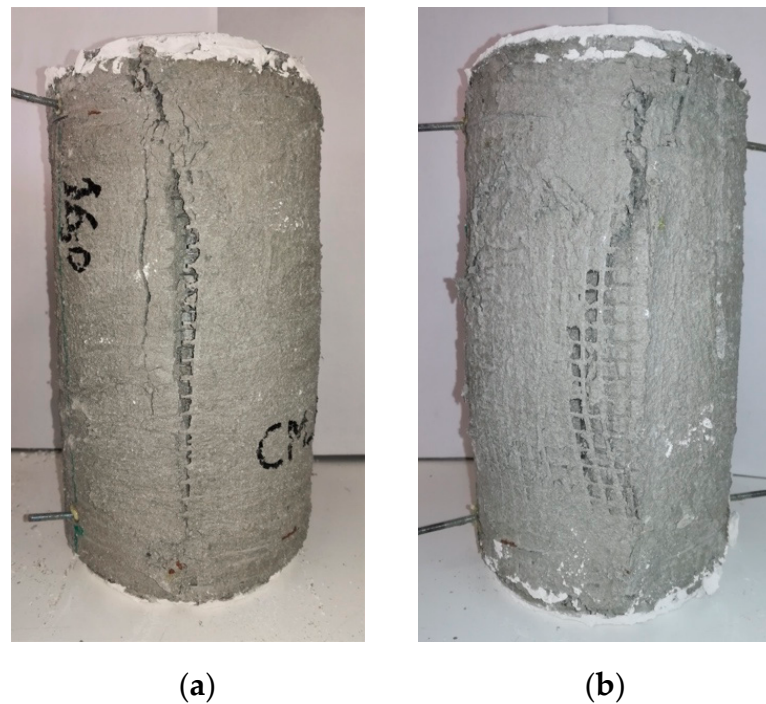


Figure 15. Failure modes of the confined specimens exhibiting debonding of the TRM jackets from mixture (a) CM_1L and (b) R75_1L.

4. Conclusions

This study experimentally investigated the mechanical performance of TRM-confined rubberised concrete subjected to monotonic axial loading. Cylindrical specimens from one reference plain concrete mixture and four rubberised concrete mixtures with increasing rubber content were tested. In total, 70 specimens were tested both unconfined and confined with either one or two TRM layers. As a result, compressive strength, stress–strain behaviour and toughness were assessed for each mixture and confinement scheme. The main conclusions are presented below:

- Slump and entrained air increased up to 6.67% and 39%, respectively, when the rubber content increased to 31.5% of the total volume. Further increase in the rubber content reduced the workability. The density of hardened concrete was reduced up to 22%.
- Replacement of mineral aggregates with rubber particles in the concrete mixture resulted in a decrease in concrete compressive strength. The reduction was 44% for rubber content of 10.5% and reached up to 78% for rubber content 42% of the total aggregate volume. Confinement increased compressive strength up to 35.5% and 38.1% for one and two TRM layers, respectively.

Statistical analysis revealed that the rubber content and the application of confinement are significant parameters affecting the compressive strength. However, the number of confinement layers was found of no significance.

- Stress–strain curves became smoother at the peak, especially when the rubber content increased, while exhibiting increased axial strain capacity post-peak. The behaviour of confined rubberised concrete with one and two TRM layers was similar, but the latter seemed to further enhance the axial strain capacity.
- Ultimate axial strain of the mixture with the highest rubber content (42%) was less than that of the mixture with the second highest rubber content (31.5%) when confined. This could be attributed to the very high rubber content of the former, indicating the importance of the rubber content optimisation.
- For unconfined specimens, plain concrete mixtures exhibited the highest toughness, because the significant loss of strength prevented rubberised concrete from achieving

a high energy absorption capacity. Confined rubberised concrete indicated increased toughness up to 169.1% and 256.9% for one and two TRM layers, respectively, while confinement with two TRM layers was more effective, and specimens exhibited a ductile-like behaviour.

- Rubberised concrete indicated a less brittle failure mode than plain concrete, accompanied by increased lateral dilation, which was even more pronounced as the rubber content increased.

Overall, the above results indicate that rubberised concrete when confined with TRM jackets can exhibit improved axial strain capacity post-peak and toughness. These properties could be proved helpful in applications where high deformability is required, such as members that are subjected to seismic loads. Additionally, the use of a recycled material (rubber particles) promotes sustainability in construction as part of a goal to reduce greenhouse gas emissions. Future research could focus on the optimisation of the rubber content and gradation in the concrete mixtures. Further examination of TRM systems is also recommended in order to evaluate the influence of the mortar's properties as well as the different textiles' mechanical properties and geometries.

Author Contributions: Conceptualization, L.N.K. and C.G.P.; Data curation, I.S.; Investigation, I.S.; Supervision, L.N.K. and C.G.P.; Validation, L.N.K. and C.G.P.; Writing—original draft, I.S.; Writing—review and editing, L.N.K. and C.G.P. All authors have read and agreed to the published version of the manuscript.

Funding: This research received no external funding.

Data Availability Statement: The data presented in this study are available on request from the corresponding authors.

Acknowledgments: The authors wish to thank Despina Tata for her assistance with the statistical analysis, the technical staff member Alekos Koutselinis and the undergraduate student Christos Agathopoulos for their assistance in part of the lab activities. Sika Hellas ABEE is also gratefully acknowledged for providing materials used in the current research.

Conflicts of Interest: The authors declare no conflict of interest.

References

1. European Commission. Internal Market, Industry, Entrepreneurship and SMEs. Buildings and Construction. Available online: https://ec.europa.eu/growth/industry/sustainability/buildings-and-construction_en (accessed on 8 December 2021).
2. Directive (EC) 98/2008 of the European Parliament and the Council of 19 November 2008 on Waste and Replacing Certain Directives. Available online: <https://eur-lex.europa.eu/eli/dir/2008/98/oj> (accessed on 8 December 2021).
3. European Commission. Circular Economy—Principles for Building Design. Available online: <https://ec.europa.eu/docsroom/documents/39984> (accessed on 8 December 2021).
4. Mavroulidou, M.; Figueiredo, J. Discarded tyre rubber as concrete aggregate: A possible outlet for used tyres. *Glob. NEST J.* **2013**, *12*, 359–367.
5. Lashari, A.R.; Ali, Y.; Buller, A.S.; Memon, N.A. Effects of partial replacement of fine aggregates with crumb rubber on skid resistance and mechanical properties of cement concrete pavements. *Int. J. Pavement Eng.* **2022**, *1*–11. [[CrossRef](#)]
6. Sienkiewicz, M.; Kucinska-Lipka, J.; Janik, H.; Balas, A. Progress in used tyres management in the European Union: A review. *Waste Manag.* **2012**, *32*, 1742–1751. [[CrossRef](#)] [[PubMed](#)]
7. European Tyre and Rubber Manufacturers' Association (ETRMA). Europe—91% of all End of Life Tyres Collected and Treated in 2018. Available online: <https://www.etrma.org/library/europe-91-of-all-end-of-life-tyres-collected-and-treated-in-2018/> (accessed on 8 December 2021).
8. Korniejenko, K.; Kozub, B.; Bağ, A.; Balamurugan, P.; Uthayakumar, M.; Furtos, G. Tackling the circular economy challenges—Composites recycling: Used tyres, wind turbine blades, and solar panels. *J. Compos. Sci.* **2021**, *5*, 243. [[CrossRef](#)]
9. Eldin, N.N.; Senouci, A.B. Rubber-Tire Particles as Concrete Aggregate. *J. Mater. Civ. Eng.* **1993**, *5*, 478–496. [[CrossRef](#)]
10. Topçu, I.B. The properties of rubberized concretes. *Cem. Concr. Res.* **1995**, *25*, 304–310. [[CrossRef](#)]
11. Toutanji, H.A. The use of rubber tire particles in concrete to replace mineral aggregates. *Cem. Concr. Compos.* **1996**, *18*, 135–139. [[CrossRef](#)]
12. Siddika, A.; Mamun, M.A.A.; Alyousef, R.; Amran, Y.H.M.; Aslani, F.; Alabduljabbar, H. Properties and utilizations of waste tire rubber in concrete: A review. *Constr. Build. Mater.* **2019**, *224*, 711–731. [[CrossRef](#)]

13. Ataria, R.B.; Wang, Y.C. Mechanical Properties and Durability Performance of Recycled Aggregate Concrete Containing Crumb Rubber. *Materials* **2022**, *15*, 1776. [CrossRef]
14. Su, H.; Yang, J.; Ling, T.-C.; Ghataora, G.S.; Dirar, S. Properties of concrete prepared with waste tyre rubber particles of uniform and varying sizes. *J. Clean. Prod.* **2015**, *91*, 288–296. [CrossRef]
15. Raffoul, S.; Garcia, R.; Pilakoutas, K.; Guadagnini, M.; Medina, N.F. Optimisation of rubberised concrete with high rubber content: An experimental investigation. *Constr. Build. Mater.* **2016**, *124*, 391–404. [CrossRef]
16. Khaloo, A.R.; Dehestani, M.; Rahmatabadi, P. Mechanical properties of concrete containing a high volume of tire–rubber particles. *Waste Manag.* **2008**, *28*, 2472–2482. [CrossRef]
17. Segre, N.; Joeques, I. Use of tire rubber particles as addition to cement paste. *Cem. Concr. Res.* **2000**, *30*, 1421–1425. [CrossRef]
18. Youssf, O.; Mills, J.E.; Hassanli, R. Assessment of the mechanical performance of crumb rubber concrete. *Constr. Build. Mater.* **2016**, *125*, 175–183. [CrossRef]
19. Papakonstantinou, C.G.; Tobolski, M.J. Use of waste tire steel beads in Portland cement concrete. *Cem. Concr. Res.* **2006**, *36*, 1686–1691. [CrossRef]
20. Alsaif, A.; Koutas, L.; Bernal, S.A.; Guadagnini, M.; Pilakoutas, K. Mechanical performance of steel fibre reinforced rubberised concrete for flexible concrete pavements. *Constr. Build. Mater.* **2018**, *172*, 533–543. [CrossRef]
21. Alsaif, A.; Alharbi, Y.R. Strength, durability and shrinkage behaviours of steel fiber reinforced rubberized concrete. *Constr. Build. Mater.* **2022**, *345*, 128295. [CrossRef]
22. Noaman, A.T.; Abu Bakar, B.H.; Akil, H.M. Experimental investigation on compression toughness of rubberized steel fibre concrete. *Constr. Build. Mater.* **2016**, *115*, 163–170. [CrossRef]
23. Raffoul, S.; Garcia, R.; Escolano-Margarit, D.; Guadagnini, M.; Hajirasouliha, I.; Pilakoutas, K. Behaviour of unconfined and FRP-confined rubberised concrete in axial compression. *Constr. Build. Mater.* **2017**, *147*, 388–397. [CrossRef]
24. Youssf, O.; Hassanli, R.; Mills, J.E. Mechanical performance of FRP-confined and unconfined crumb rubber concrete containing high rubber content. *J. Build. Eng.* **2017**, *11*, 115–126. [CrossRef]
25. Chan, C.W.; Yu, T.; Zhang, S.S.; Xu, Q.F. Compressive behaviour of FRP-confined rubber concrete. *Constr. Build. Mater.* **2019**, *211*, 416–426. [CrossRef]
26. Bompa, D.V.; Elghazouli, A.Y. Stress–strain response and practical design expressions for FRP-confined recycled tyre rubber concrete. *Constr. Build. Mater.* **2020**, *237*, 117633. [CrossRef]
27. Hassanli, R.; Youssf, O.; Vincent, T.; Mills, J.E.; Manalo, A.; Gravina, R. Experimental study on compressive behavior of FRP-confined expansive rubberized concrete. *J. Compos. Constr.* **2020**, *24*, 04020034. [CrossRef]
28. Wang, Z.; Hajirasouliha, I.; Guadagnini, M.; Pilakoutas, K. Axial behaviour of FRP-confined rubberised concrete: An experimental investigation. *Constr. Build. Mater.* **2021**, *267*, 121023. [CrossRef]
29. Youssf, O.; ElGawady, M.A.; Mills, J.E. Static cyclic behaviour of FRP-confined crumb rubber concrete columns. *Eng. Struct.* **2016**, *113*, 371–387. [CrossRef]
30. Moustafa, A.; Ghenni, A.; ElGawady, M.A. Shaking-Table Testing of High Energy–Dissipating Rubberized Concrete Columns. *J. Bridge Eng.* **2017**, *22*, 04017042. [CrossRef]
31. Elghazouli, A.Y.; Bompa, D.V.; Xu, B.; Ruiz-Teran, A.M.; Stafford, P.J. Performance of rubberised reinforced concrete members under cyclic loading. *Eng. Struct.* **2018**, *166*, 526–545. [CrossRef]
32. Cao, Y.; Li, L.; Liu, M.; Wu, Y. Mechanical behavior of FRP confined rubber concrete under monotonic and cyclic loading. *Compos. Struct.* **2021**, *272*, 114205. [CrossRef]
33. Koutas, L.N.; Tetta, Z.; Bournas, D.A.; Triantafillou, T.C. Strengthening of Concrete Structures with Textile Reinforced Mortars: State-of-the-Art Review. *J. Compos. Constr.* **2019**, *23*, 03118001. [CrossRef]
34. Triantafillou, T.C.; Papanicolaou, C.G.; Zissimopoulos, P.; Laouderkis, T. Concrete Confinement with Textile-Reinforced Mortar Jackets. *ACI Struct. J.* **2006**, *103*, 28–37.
35. Ombres, L. Concrete confinement with a cement based high strength composite material. *Compos. Struct.* **2014**, *109*, 294–304. [CrossRef]
36. Di Ludovico, M.; Prota, A.; Manfredi, G. Structural Upgrade Using Basalt Fibers for Concrete Confinement. *J. Compos. Constr.* **2010**, *14*, 541–552. [CrossRef]
37. Bournas, D.A.; Lontou, P.V.; Papanicolaou, C.G.; Triantafillou, T.C. Textile-Reinforced Mortar versus Fiber-Reinforced Polymer Confinement in Reinforced Concrete Columns. *ACI Struct. J.* **2007**, *104*, 740.
38. Greek Concrete Technology Code 2016. Ministerial Decision of the ECO. 3328, GG. 1561/b/02.06.2016. Available online: https://www.ggde.gr/index.php?option=com_k2&view=item&id=529:%CE%BA%CE%B1%CE%BD%CE%BF%CE%BD%CE%B9%CF%83%CE%BC%CF%8C%CF%82-%CF%84%CE%B5%CF%87%CE%BD%CE%BF%CE%BB%CE%BF%CE%B3%CE%AF%CE%B1%CF%82-%CF%83%CE%BA%CF%85%CF%81%CE%BF%CE%B4%CE%AD%CE%BC%CE%B1%CF%84%CE%BF%CF%82-%CE%BA%CF%84%CF%83-2016&Itemid=326 (accessed on 9 August 2022).
39. EN 12390-2:2019; Testing Hardened Concrete—Part 2: Making and Curing Specimens for Strength Tests. CEN (European Committee for Standardization): Brussels, Belgium, 2019.
40. EN 12350-2:2019; Testing Fresh Concrete—Part 2: Slump Test. CEN (European Committee for Standardization): Brussels, Belgium, 2019.
41. EN 12350-7:2019; Testing Fresh Concrete—Part 7: Air Content—Pressure Methods. CEN (European Committee for Standardization): Brussels, Belgium, 2019.

-
42. *EN 12390-7:2019*; Testing Hardened Concrete—Part 7: Density of Hardened Concrete. CEN (European Committee for Standardization): Brussels, Belgium, 2019.
 43. *EN 1015-11:2019*; Methods of Test for Mortar for Masonry—Part 11: Determination of Flexural and Compressive Strength of Hardened Mortar. CEN (European Committee for Standardization): Brussels, Belgium, 2019.